Development of cesium laser resonance ionization schemes for PLASEN experiment*

Yangfan Guo (郭洋帆)¹ Zhou Yan (严周)¹ Xiaofei Yang (杨晓菲)¹ Shaojie Chen (陈少杰)¹ Wencong Mei (梅文聪)¹ Hanrui Hu (胡晗睿)¹ Yinshen Liu (刘寅绅)¹ Dongyang Chen (陈冬阳)¹ Chen Zhang (张臣)¹ Tianxu Gao (高天旭)¹ Yipin Jing (景一品)² Yanlin Ye (叶沿林)¹

¹School of Physics and State Key Laboratory of Nuclear Physics and Technology, Peking University, Beijing 100871, China
²College of Physics, Jilin University, Changchun 130012, China

Abstract: To study the nuclear properties and deformation of neutron-rich cesium isotopes in their ground and isomeric states at the Beijing Rare Isotope Beam Facility (BRIF), optimal resonance ionization schemes and experimental conditions must be predetermined. In this study, we evaluated several three-step laser resonance ionization schemes for cesium atoms by accessing their ionization efficiency and spectral resolution under varying measurement conditions using high-resolution and high-sensitivity collinear resonance ionization spectroscopy system. Hence, we identified the currently most efficient resonance ionization scheme and optimal experimental conditions, achieving an overall measurement efficiency of 1: 400 with a spectral resolution of about 100 MHz. Under this condition, the extracted hyperfine structure parameters of ¹³³Cs showed excellent agreement with previously reported values. This study establishes a solid foundation for the forthcoming online measurement of neutron-rich cesium isotopes at BRIF.

Keywords: hyperfine structure, nuclear properties, laser spectrosocpy, resonance ionization

I. INTRODUCTION

The fundamental properties of exotic nuclei provide crucial insights into nuclear structure and nucleon-nucleon interactions. Investigation of nuclear properties across different mass regions of the nuclear chart aids in uncovering novel structural phenomena, testing theoretical models, and refining our understanding of the nuclear force [1-7]. By measuring hyperfine structure (HFS) and isotope shift in atomic, ionic, or even molecular spectra [3, 8, 9] via laser spectroscopy technique, nuclear spins, magnetic moments, electric quadrupole moments, and charge radii can be precisely determined in a nuclearmodel-independent way. In recent years, laser spectroscopy has emerged as a powerful tool for probing nuclear properties of exotic nuclei and has been widely implemented at numerous radioactive ion beam (RIB) facilities worldwide, providing essential experimental benchmarks for nuclear theory and advancing our understanding of exotic nuclear phenomena [10-12].

Collinear laser spectroscopy (CLS) is one of the most widely used laser spectroscopy techniques [13–16]. By

overlapping the lasers and fast ion beam collinearly or anti-collinearly, the doppler broadening effect associated with the energy spread of the ion beam can be significantly suppressed, achieving a high resolution of approximately 10¹⁻² MHz [17]. The HFS spectra of unstable nuclei can be measured via CLS technique using two approaches: laser-induced fluorescence (LIF) [13, 15, 16] and resonance ionization spectroscopy (RIS) [14, 18]. LIF approach measures HFS spectra by detecting fluorescence photons emitted from an excited state of the atoms or ions as a function of the probing laser frequency. However, the scattered laser light and thermal noise of the detecting photomultiplier tube result in a high background rate in the measured HFS spectra, limiting the sensitivity of CLS experiment using the LIF approach. Therefore, by additionally employing one or two more lasers to overlap (anti-)collinearly with the atom beams and to ionize them, the RIS approach can measure the HFS spectra with a high resolution and high sensitivity [14, 18].

To study nuclear properties and exotic structure of unstable nuclei at radioactive ion beam facilities in China,

Received 31 March 2025; Accepted 25 July 2025; Published online 26 July 2025

^{*} Supported by National Key R&D Program of China (2023YFE0101600, 2023YFA1606403, 2022YFA1605100), National Natural Science Foundation of China (12027809, 12350007)

[†] E-mail: xiaofei.yang@pku.edu.cn

^{©2025} Chinese Physical Society and the Institute of High Energy Physics of the Chinese Academy of Sciences and the Institute of Modern Physics of the Chinese Academy of Sciences and IOP Publishing Ltd. All rights, including for text and data mining, AI training, and similar technologies, are reserved.

e.g., Beijing Rare Isotope Beam Facility (BRIF) [19], a CLS system with LIF detection was first developed [20, 21]. The CLS system exhibited limited experimental efficiency as expected. To achieve higher efficiency measurements, this system was further updated into a collinear resonance ionization spectroscopy system (PLASEN, Precision LAser Spectroscopy for Exotic Nuclei) by implementing the radiofrequency quadrupole (RFQ) coolerbuncher and RIS approach [22-24]. This led to an overall efficiency of 1: 200 with a spectral resolution of ~100 MHz (FWHM) for ^{85,87}Rb isotopes. The system is expected to be installed at BRIF to study the nuclear properties of unstable nuclei in the medium-mass region of the nuclear chart produced from the fission of actinide, in particular the isotopes around Z = 55 and N = 90. This region has long been theoretically predicted to exhibit potential deformation and octupole correlations [25], which however, have not been clearly observed in the groundstate properties—such as masses and half-lives—of neutron-rich Xe (Z = 54), Cs (Z = 55) and Ba (Z = 56) [26, 27]. Therefore, further measurements of charge radii and moments in neutron-rich Cs isotopes using laser spectroscopy will provide more insights into deformation in this mass region.

The isotopes under investigation are ¹⁴⁷⁻¹⁵⁰Cs, which are expected to be produced at BRIF with a yield greater than 10² particles per second (pps). Thus, to ensure successful laser spectroscopy measurements of unstable Cs isotopes, optimal resonance ionization schemes and experimental conditions must be predetermined.

In this study, we tested several three-step laser resonance ionization schemes for cesium atoms under relatively optimized experimental conditions of 80% neutralization efficiency and 80% overall ion beam transmission efficiency using the PLASEN system. We evaluated the ionization efficiency and spectral resolution of these

candidate schemes and identified the most efficient scheme that achieved an overall measurement efficiency of 1: 400 with a spectral resolution of approximately 100 MHz. An HFS spectrum of ¹³³Cs was measured under this condition, and thereby, the extracted HFS parameters showed excellent agreement with those reported in literature. This study establishes a solid foundation for the forthcoming online measurements of neutron-rich cesium isotopes at BRIF.

II. EXPERIMENT TECHNIQUE

The experimental setup, PLASEN, used for this measurement is illustrated in Fig. 1(a). More details on the PLASEN system can be found in Ref. [24]. The entire experiment begins with the production of a continuous ¹³³Cs ion beam from a surface ion source. These ions were extracted and accelerated to 30 keV before being injected into the RFQ cooler and buncher [23, 28]. With the RFQ, the ion beam was cooled and accumulated for 10 ms before it was released as short bunches with a temporal width of approximately 2 µs and at a repetition rate 100 Hz. The ion bunches were then re-accelerated to 30 keV. The cooling process inside RFQ reduced the potential energy spread of the ion beam and improved the ion beam profile by reducing the beam emittance [23]. To avoid any space charge effects, the total ion beam current injected into the RFQ was limited to below 1 pA using a modulated ion beam gate. During this Cs test experiment, the transmission efficiency of the RFQ was approximately 60%, which was verified using the Faraday cups before and after RFQ [24].

The bunched Cs ion beam with a higher quality beam profile was subsequently deflected into the collinear beamline via a dipole magnet. By using the ion optics consisting of electrostatic quadrupole triplet (QT) lenses,

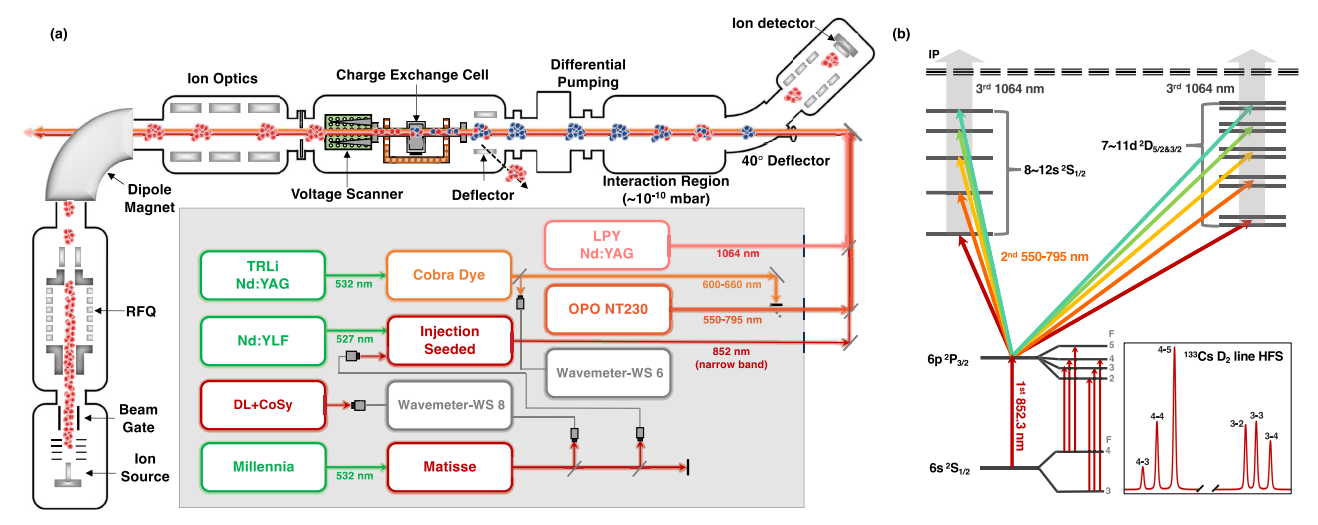


Fig. 1. (color online) (a) A schematic view of the entire experimental setup and laser systems used for study work. (b) Resonance ionization schemes of Cs I being tested in this study.

x-y correction plates and deflector plates, the bunched Cs beam was further optimized and delivered into the end of the PLASEN setup. Using the bunched Cs ion beam, the overall transmission efficiency of the PLASEN setup exceeded 80%, and it was verified using the Faraday cups after the RFQ and at the end of the PLASEN [24]. Within the collinear beamline, the ion beam underwent neutralization with sodium vapor in the charge exchange cell (CEC). Any residual unneutralized ions were removed by the deflector plates positioned after the CEC. The general neutralization efficiency was measured as 80% for Cs ions. The neutralized Cs atoms were delivered into the interaction region (IR). Here, the Cs atomic beam was spatially overlapped and temporally synchronized with three pulsed laser beams (see Sec. III for details) and simultaneously resonantly ionized. To suppress any possible collisional ionization, IR was maintained at an ultra-high vacuum of 10⁻¹⁰ mbar, achieved via a differential pumping system that isolates the IR from the 10⁻⁸ mbar environment inside the CEC [22].

Following resonance ionization, the ions were guided toward MagneTOF ion detector via 40° electrostatic bender plates and a set of QT lenses. By scanning the frequency of the probing laser (the first step laser as detailed below in Sec. III), the HFS spectra were obtained by measuring the detected ion rates as a function of the laser frequency [29].

III. RESONANCE IONIZATION SCHEME TEST FOR Cs ATOM

A study of the nuclear properties of neutron-rich Cs isotopes is already planned at BRIF facility. To obtain an optimal experimental condition for the online experiment, the testing of all the potential resonance ionization schemes in advance is indispensable. The potential candidate schemes are shown in Fig. 1(b). Here, we select D₂ $(5p^66s^2S_{1/2} \rightarrow 5p^66p^2P_{3/2}^{\circ}, 851.2 \text{ nm})$ transition as the first resonance step for the HFS spectrum measurement of ¹³³Cs. Although the electric quadrupole HFS constant $B_{\rm u}$ of the D₂ transition of ¹³³Cs is relatively low, the $B_{\rm u}$ values for unstable cesium isotopes are large enough to be extracted from the HFS spectra measured with CLS according to previous laser spectroscopy studies [30, 31]. Therefore, using D₂ transition allows us to simultaneously extract the nuclear spins, magnetic moments, quadrupole moments, and charge radii of Cs isotopes.

All the involved laser system used for the resonance ionization schemes, shown in Fig. 1(b), are presented in Fig. 1(a). As the D_2 line is used for the HFS measurement, the laser used for this $5p^66s^2S_{1/2} \rightarrow 5p^66p^2P_{3/2}^\circ$ step is required to be narrow-band to resolve the HFS. Here, we employed an injection-seeded laser with a linewidth of less than 20 MHz at a 100 Hz repetition rate [32]. The system was seeded by a continuous-wave nar-

row-band Ti:Sa laser and pumped by a 527 nm pulsed Nd:YLF laser. A high-precision wavemeter was used to ensure long-term frequency stability. This wavemeter was continuously calibrated in real time by a tunable diode laser, whose frequency was locked to a HFS transition of ⁸⁷Rb in a temperature-controlled vapor cell. To obtain optimal resonance ionization efficiency, multiple transitions from $5p^66p^2P_{3/2}^{\circ}$ to $5p^6nd^2D_{3/2,5/2}$ (n=7-11) or $5p^6ns^2S_{1/2}$ (n = 8 - 12) were tested for the second excitation step, covering a laser wavelength of 550-795 nm. A pulsed dye laser pumped by a 532 nm Nd:YAG laser, capable of delivering 100 Hz pulsed laser beams with a power of 20 mJ, was used for this step. Additionally, an OPO laser (NT230-100, EKSPLA) was adopted for the second resonance step due to to its broad wavelength tuning range (192-2600 nm) and relatively large linewidth (3 cm⁻¹). A wavelenght of 1064 nm for the third non-resonant ionization step was produced by a Nd:YAG laser, which provides a high laser power of up to 100 mJ, which is essential for efficient ionization while minimizing laser induced background ion counts.

In this test, the high-power pulsed dye laser at 621 nm matched $5p^66p^2P_{3/2}^{\circ} \rightarrow 5p^68d^2D_{3/2}$ transition. This laser was initially used for the second-step excitation to find the RIS signal. Based on this RIS signal, we then optimized the laser power, laser path, ion beam transportation, and timing of the laser pulses to maximize efficiency. Under this optimal experimental conditions, we switched to OPO laser for the second step and compared the resonance ionization efficiencies at the maximum available power by scanning OPO wavelength from 550 nm to 795 nm, covering all the second step transitions. The count rates obtained with different second steps were recorded and compared under two different conditions (full power and lower power for the first step), as shown in Table 1 and Fig. 2. In the full power case, the ionization efficiency was maximized, but at the cost of poor spectral resolution (1 ~2 GHz) due to the possible power broadening. The results shown in Table 1 and Fig. 2 indicate that $5p^67d^2D_{5/2}$ state for the second step exhibits the highest efficiency. However, to extract the nuclear properties of spins, magnetic moments, quadrupole moments, and charge radii of Cs isotopes with high accuracy, an HFS spectral resolution of approximately 100 MHz or even lower is prerequisite. Therefore, to obtain a compromised condition for high resolution and high efficiency, the first-step laser power was reduced to obtain an HFS spectrum with a resolution of ~100 MHz. Under this condition, any of the transitions to the "nd D" states can be used for efficient resonance ionization; however, n = 8 $(5p^68d^2D_{5/2})$ state is slightly better than others. It is worth noting that the achieved efficiency under the fullpower condition is approximately three times higher than that under the lower-power condition. Although the highpower measurements are inadequate for determining the

0.984

0.060

0.885

0.045

0.750

 $6p^2P_{3/2}^{\circ} \rightarrow 9d^2D_{3/2,5/2}^{\circ}$

 $6p\ ^2P_{3/2}^{\circ} \rightarrow 11s\ ^2S_{1/2}$

 $6p^2P_{3/2}^{\circ} \rightarrow 10d^2D_{3/2,5/2}^{\circ}$

 $6p\ ^2P_{3/2}^{\circ} \rightarrow 12s\ ^2S_{1/2}$

 $6p^2P_{3/2}^{\circ} \rightarrow 11d^2D_{3/2,5/2}^{\circ}$

Ionization

585.15

574.97

564.06

557.76

550.72

1064

Transition	Wavenumber /cm ⁻¹	Counts (×10 ³ /min) (full power) ^a	Relative Counts (full power) ^a	Counts (×10 ³ /min) (lower power) ^b	Relative Counts (lower power) ^b
$6s^2S_{3/2} \rightarrow 6p^2P_{3/2}^{\circ}$	852.35	_	-	-	-
$6p\ ^2P_{3/2}^{\circ} \rightarrow 8s\ ^2S_{1/2}$	794.94	14.34(12)	0.104	5.34(7)	0.133
$6p\ ^2P^{\circ}_{3/2} \to 7d\ ^2D_{3/2}$	698.84	89.40(30)	0.650	32.82(18)	0.815
$6p\ ^2P^{\circ}_{3/2} \to 7d\ ^2D_{5/2}$	697.82	137.52(37)	1.000	39.48(20)	0.981
$6p\ ^2P_{3/2}^{\circ} \rightarrow 9s\ ^2S_{1/2}$	659.11	11.22(11)	0.082	4.20(6)	0.104
$6p\ ^2P^{\circ}_{3/2} \to 8d\ ^2D_{3/2}$	622.19	97.80(31)	0.711	36.72(19)	0.912
$6p\ ^2P^{\circ}_{3/2} \to 8d\ ^2D_{5/2}$	621.74	134.16(37)	0.976	40.26(20)	1.000
$6p\ ^2P_{3/2}^{\circ} \rightarrow 10s\ ^2S_{1/2}$	603.83	6.42(8)	0.047	2.94(5)	0.073

0.669

0.029

0.553

0.017

0.540

39.60(20)

2.40(5)

35.64(19)

1.80(4)

30.18(17)

Table 1. Summary of test results and information for second-step in the resonance ionization schemes listed in Fig. 1(b)

91.98(30)

4.02(6)

76.08(28)

2.34(5)

74.22(27)

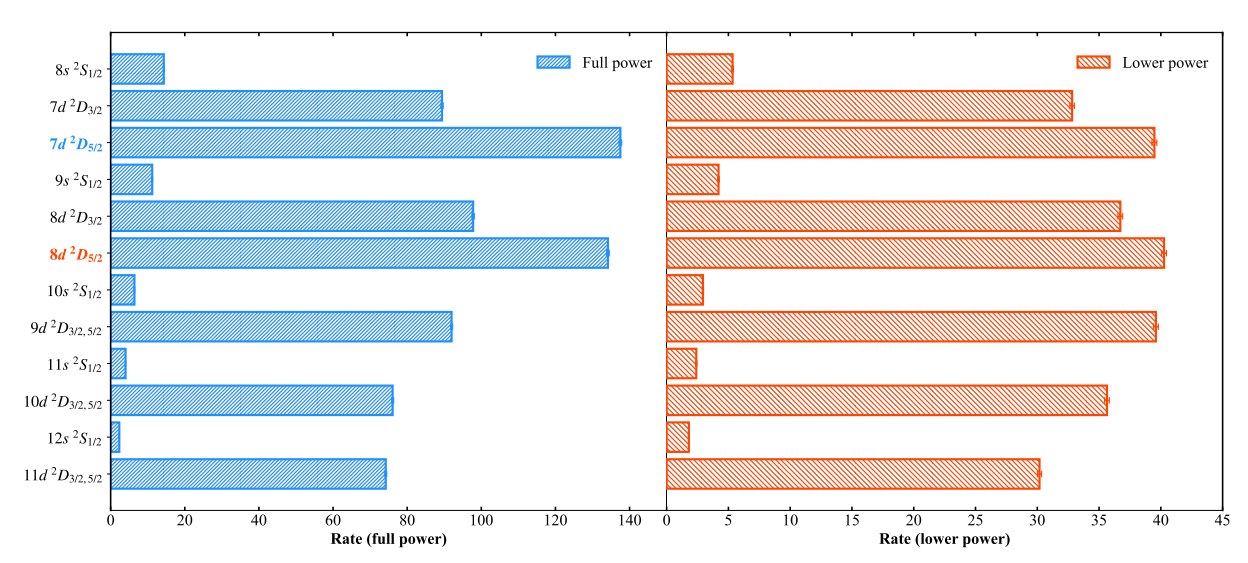


Fig. 2. (color online) RIS count rate for different upper state of the second-step transition, obtained on the condition of the first-step laser at full power (left panel: blue) and at a reduced power (right panel: red). The states used for achieving the highest efficiency are highlighted in bold and with the corresponding color.

nuclear spins and quadrupole moments, they still allow us to study more exotic isotopes with lower production yields, enabling the extraction of charge radii and magnetic moments. Nevertheless, for isotopes with higher production yields, we will primarily perform HFS measurements under lower-power condition to determine the HFS constants with high accuracy.

Based on the results, we identified that the most suitable resonance ionization scheme for high resolution and high efficiency HFS spectrum measurement for Cs isotopes is $5p^66s\ ^2S_{1/2} \rightarrow 5p^66p\ ^2P^{\circ}_{3/2} \rightarrow 5p^68d\ ^2D_{5/2} \rightarrow IP$. Finally, by using this identified scheme, we optimized the experimental conditions one more time, including optimization of the line shape by varying laser power, laser and ion beam overlapping, and relative delaying of the laser pulses. Finally, we measured the HFS spectra of D₂ line for ¹³³Cs shown in Fig. 3(a) with an efficiency of 1: 400 and a spectral resolution of ~100 MHz, which is considered based on the relative delaying of the laser pulses shown in Fig. 3(b). The efficiency was evaluated from the

Relative counts obtained with the first-step laser at full power. Relative counts obtained with the first-step laser at a reduced power to obtain a spectral resolution of ~100 MHz. ^c OPO laser is unable to resolve the two close atomic levels.

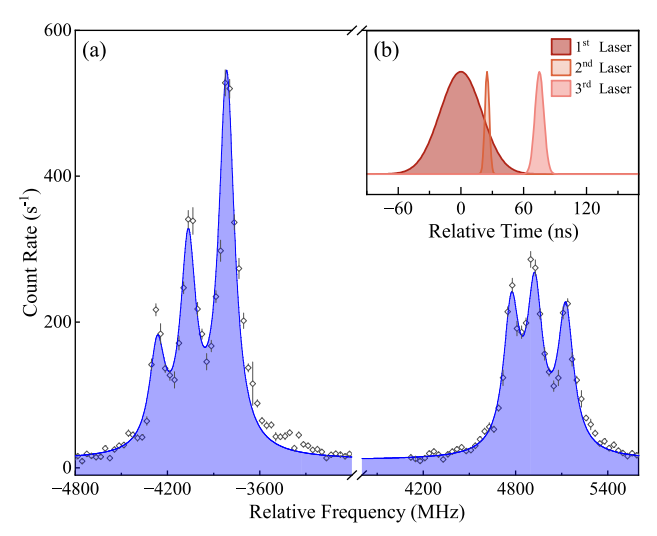


Fig. 3. (color online) (a) HFS spectrum of 133 Cs obtained with an efficiency of 1: 400 and a resolution of \sim 100 MHz (FWHM). (b) The optimized timing sequences of the three-step laser pulses. See text for further details.

detected resonance ionization counts and ion beam intensity after the RFQ, which includes the efficiencies of ion beam transmission, neutralization, resonance ionization, and detection. Based on this efficiency, it can be estimated that for an isotope with a production of 100 pps along with an isobar contamination of 10⁴ pps, a full HFS spectrum can be measured within a reasonable experimental time of approximately 16 h [24].

The HFS spectrum of 133 Cs shown in Fig. 3(a) was analyzed using a Voigt profile and a χ^2 -minimization approach implemented in SATLAS2 package [34]. The extracted magnetic dipole and electric quadrupole HFS parameters A and B are in excellent agreement with the literature values [33] shown in Table 2.

This test experiment realized high-resolution and high-sensitivity HFS spectrum measurements of ¹³³Cs, and it sets an important foundation for the upcoming online experiment for the study of neutron-rich ¹⁴⁷⁻¹⁵⁰Cs iso-

Table 2. Hyperfine structure constants of ¹³³Cs measured in this study and taken from literature.

	A_1	A_{u}	B_{u}
Exp.	2297.7(8)	50.45(36)	-2.6(21)
Ref. [30] ^a	2298.3(2)	50.15(8)	-1.35(80)
Ref. [33]b	2298.1579425°	50.28827(23)	-0.4934(17)

^a The reference values are measured using collinear laser spectroscopy [30]. ^b The reference values are taken from Ref. [33], which summarizes the most precise atomic physics measurements for stable ¹³³Cs. ^c Exact by definition, as the SI second is defined by the hyperfine splitting of the $6S_{1/2}$ state of ¹³⁵Cs..

topes at BRIF.

IV. SUMMARY AND OUTLOOK

In this study, a systematic investigation of the three-step laser resonance ionization schemes of cesium was conducted using PLASEN system. A three step scheme $5p^66s^2S_{1/2} \rightarrow 5p^66p^2P_{3/2}^{\circ} \rightarrow 5p^68d^2D_{5/2} \rightarrow$ IP was identified as the most suitable for high-resolution and high-efficiency resonance ionization laser spectroscopy measurement. Using this scheme, we further optimized experimental condition, resulting in an HFS spectrum for $^{133}{\rm Cs}$ with an overall measurement efficiency of 1: 400 while maintaining a spectral resolution of approximately 100 MHz (FWHM). The extracted HFS parameters were in excellent agreement with those reported literature. This study establishes a solid experimental foundation for examining neutron-rich cesium isotopes beyond N=90 at BRIF.

As ISOL target development progresses at BRIF [19] and with the construction of next-generation RIB facilities in China [35], a broader range of exotic nuclei will be accessible in the near future. This study additionally demonstrates the feasibility of the PLASEN setup for systematic RIS scheme development of stable isotopes and for obtaining an optimal measurement condition prior to perform online experiment on their exotic isotopes at RIB facilities.

References

^[1] Y. L. Ye, X. F. Yang, H. Sakurai *et al.*, Nature Reviews Physics 7, 21 (2025)

^[2] W. Nörtershäuser, D. Tiedemann, M. Žáková et al., Phys. Rev. Lett. 102, 062503 (2009)

^[3] R. F. Garcia Ruiz, M. L. Bissell, K. Blaum *et al.*, Nature Physics **12**, 594 (2016)

^[4] X. F. Yang, C. Wraith, L. Xie et al., Phys. Rev. Lett. 116, 182502 (2016)

^[5] J. Karthein, C. M. Ricketts, R. F. Garcia Ruiz *et al.*, Nature Phys. **20**, 1719 (2024)

^[6] B. A. Marsh, T. D. Goodacre, S. Sels *et al.*, Nature Phys. 14, 1163 (2018)

^[7] J. Warbinek, E. Rickert, S. Raeder et al., Nature 634, 1075 (2024)

^[8] A. Koszorús, X. F. Yang, W. G. Jiang et al., Nature Phys. 17, 439 (2021)

^[9] S. M. Udrescu, A. J. Brinson, R. F. Garcia Ruiz et al., Phys. Rev. Lett. 127, 033001 (2021)

^[10] X. F. Yang, S. J. Wang, S. G. Wilkins et al., Prog. Part. Nucl. Phys. 129, 104005 (2023)

^[11] A. Koszorús, R. P. de Groote, B. Cheal et al., Eur. Phys. J. A 60, 20 (2024)

^[12] M. Block, M. Laatiaoui, S. Raeder et al., Prog. Part. Nucl. Phys. 116, 103834 (2021)

^[13] R. Neugart, J. Billowes, M. L. Bissell *et al.*, J. Phys. G: Nucl. Part. Phys. 44, 064002 (2017)

- [14] M. Athanasakis-Kaklamanakis, J. R. Reilly, A. Koszorús et al., NIMB 541, 86 (2023)
- [15] K. Minamisono, P. F. Mantica, A. Klose et al., NIMA 709, 85 (2013)
- [16] R. P. de Groote, A. de Roubin, P. Campbell *et al.*, NIMB 463, 437 (2020)
- [17] K. R. Anton, S. L. Kaufman, W. Klempt et al., Phys. Rev. Lett. 40, 642 (1978)
- [18] R. P. de Groote, A. de Roubin, P. Campbell *et al.*, NIMB **541**, 388 (2023)
- [19] T. J. Zhang, B. Q. Cui, Y. L. Lv et al., NIMB 463, 123 (2020)
- [20] S. W. Bai, X. F. Yang, S. J. Wang *et al.*, Nuclear Science and Techniques **33**, 9 (2022)
- [21] S. J. Wang, X. F. Yang, S. W. Bai et al., NIMA 1032, 166622 (2022)
- [22] P. Zhang, H. R. Hu, X. F. Yang et al., NIMB **541**, 37 (2023)
- [23] Y. S. Liu, H. R. Hu, X. F. Yang et al., arXiv: 2502.10740
- [24] H. R. Hu, Y. F. Guo, X. F. Yang et al., arXiv: 2503.20637
- [25] W. Nazarewicz, P. Olanders, I. Ragnarsson *et al.*, Nucl. Phys. A **429**, 269 (1984)
- [26] D. Atanasov, D. Beck, K. Blaum et al., J. Phys. G: Nucl.

- Part. Phys., 044004 (2017)
- [27] R. Lică, G. Benzoni, A. I. Morales et al., J. Physics G: Nucl. Part. Phys. 44, 054002 (2017)
- [28] L. Croquette, Commissioning of a Paul trap for Collinear Laser Spectroscopy of Exotic Radionuclides performed in a 30 keV MR-ToF device, Master thesis, McGill University, Montreal, February 2023
- [29] Y. C. Liu, X. F. Yang, S. W. Bai et al., Nucl. Sci. Tech. 34, 38 (2023)
- [30] C. Thibault, F. Touchard, S. Büttgenbach, *et al.*, Nucl. Phys. A 367, 1 (1981)
- [31] A. Coc, C. Thibault, F. Touchard et al., Nucl. Phys. A 468, 1 (1987)
- [32] M. Reponen, V. Sonnenschein, T. Sonoda *et al.*, NIMA 908, 236 (2018)
- [33] D. A. Steck, "Cesium D Line Data," available online at http://steck.us/alkalidata (revision 2.3.3, 28 May 2024)
- [34] W. Gins, B. van den Borne, R. P. de Groote *et al.*, Comput. Phys. Commun. 297, 109053 (2024)
- [35] X. H. Zhou, J. C. Yang, the HIAF project team, AAPPS Bulletin 32, 35 (2022)